7. Ballistic Behaviour of Aluminium Alloys Impacted by Lead Projectile

7.1. Introduction

Previous studies have explored the ballistic behaviour of different series of aluminium alloys. However, studies on the relative ballistic performance of different aluminium alloys have received less attention. In this Chapter the ballistic behaviour of 20 mm thick AA 7017 plates has been compared with that of 20 mm thick five different commercially available aluminium alloys used for armour application namely AA 2024, AA 2519, AA 5059, AA5083 and AA 6061. The details of the plates have been described in Table 2.1. All the studied aluminium plates are impacted with 7.62 mm lead projectiles. The ballistic behaviour of the different aluminium alloy plates have been interpreted in terms of their mechanical properties. The changes in the microstructure, hardness and damage pattern in post impact samples have also been studied.

7.2. Results

7.2.1. Initial microstructure

The initial microstructures of the different aluminium alloy plates are given in Fig.7.1. The microstructure of the plates exhibit grains elongated along the rolling direction.

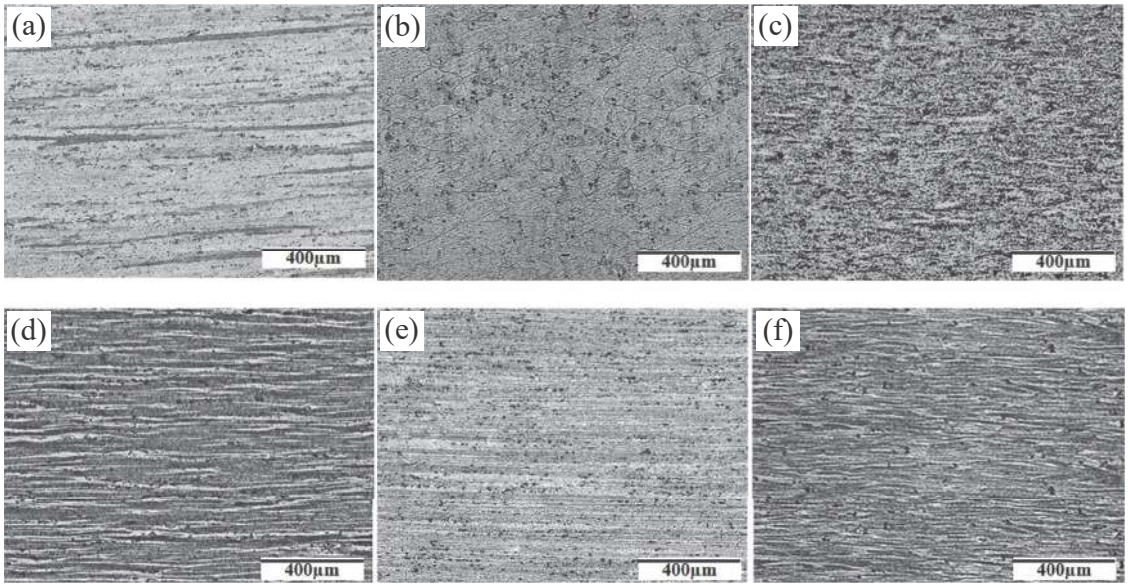

Fig. 7.1: Initial microstructure of the studied aluminium alloy plates taken along the longitudinal direction ; (a) AA 2024, (b) AA 2519, (c) AA 5059, (d) AA 5083, (e) AA 6061 and (f) AA 7017.

7.2.2. Mechanical Properties

The standard tensile and impact samples are prepared along the rolling direction of the plate to find out the mechanical properties. The representative engineering and true stress-strain curves of the different aluminium alloy plates are displayed in Fig. 7.2(a and b). The nature of the stress-strain curves of AA 2024, AA 2519, AA 6061 and AA7017 aluminium alloy plates displays typical nature of flow stress that increases continuously up to ultimate tensile strength. Serrated flow pattern was observed in the plastic deformation region of the stress-strain curves of AA 5059 and AA 5083aluminium alloy plates. It is to be noted that the serrated flow pattern starts at some critical strain and not in the beginning of plastic deformation. Observation of serrated flow pattern in AA 5083 alloys has been reported in a previous investigation [Motsi et al., 2017]. The mechanical properties of the different aluminium alloy plates are summarized in Table 7.1. The AA 7017 plate shows the highest hardness and tensile strength, whereas the AA 6061 plate displays lowest hardness

and strength values. The AA 2024 alloy plate exhibits highest value of ductility measured in terms of total elongation to failure.

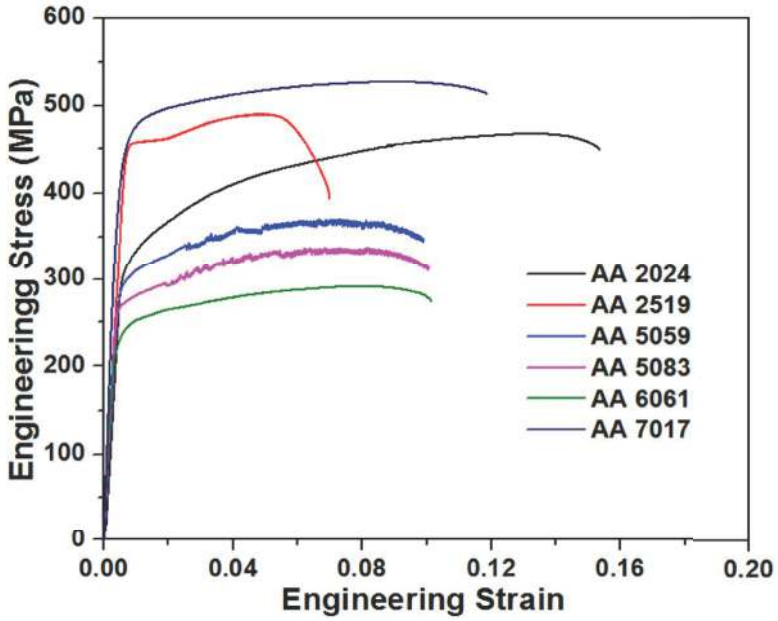

(a)

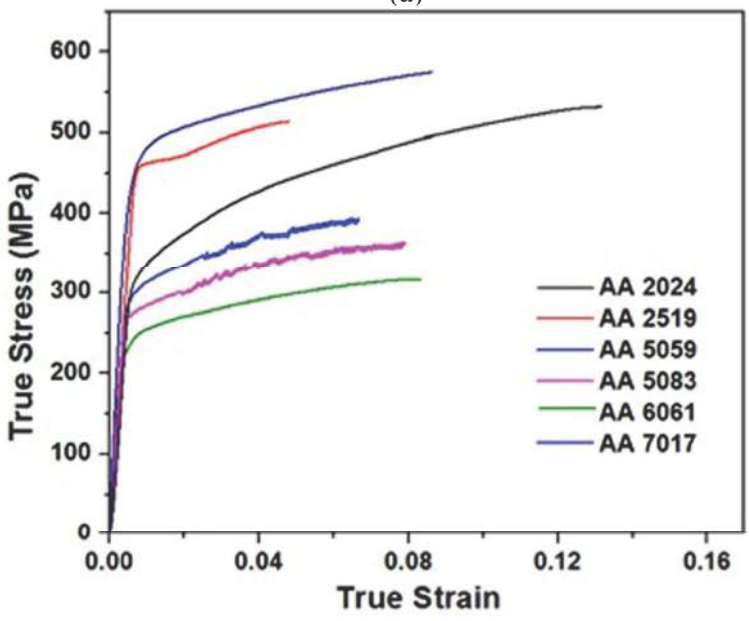

(b)

Fig. 7.2: (a) Engineering stress-strain and (b) True stress-strain curves of studied aluminium alloys.

Table 7.1: Mechanical properties of studied aluminium alloy plates.

Material	σ_{YS} (MPa)	σ_{UTS} (MPa)	Hardness (VHN)	% Elongation	CVN (J)
AA 2024	310	457	130	16.2	15
AA 2519	453	485	135	7.6	7
AA 5059	315	408	113	9.9	13
AA5083	279	346	107	10.1	14
AA 6061	250	294	87	10.4	17
AA 7017	437	513	160	11.4	9

The Charpy impact test results of different aluminium alloy plates are illustrated in Table 7.1. It can be noticed that AA 6061 and AA 2519 plates display the highest (17 J) and lowest (7 J) impact energy values respectively out of the studied alloys. The variations in fractographic features in the fracture surfaces of the broken Charpy impact specimens are depicted in Fig. 7.3. The fracture surfaces of all the aluminium alloy plates are predominantly dominated by dimples. Very fine and shallow dimples are observed in case of the fracture surface of AA 6061samples whereas coarse dimples are observed in case of AA 2519 samples. A mixture of fine and coarse dimples is observed in the fracture surfaces of other studied aluminium alloys. Presence of intermetallic precipitates can be seen in the fracture surface of all the aluminium alloys.

7.2.4. Ballistic evaluation

From the ballistic testing it is observed that all the different aluminium alloy plates are completely perforated by the projectile. The visual comparison of the different

aluminium alloy plates after ballistic impact is exhibited in Fig. 7.4. The damage mechanisms displayed by all the targets clearly indicate that the projectiles have pierced through the plates by causing ductile hole enlargement phenomenon. A close view of the front damage pattern elucidates that the material flows out to form perfect petalling damage pattern in the front side of the target plates, Fig 7.4 (b).

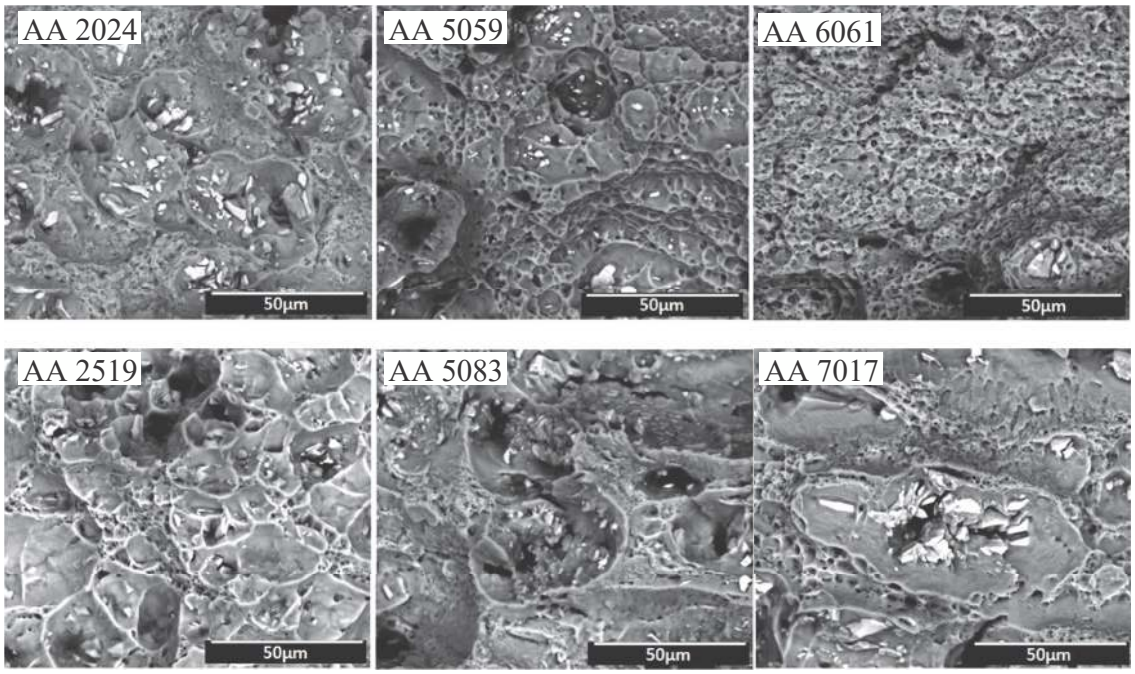

Fig. 7.3: Fractographs of Charpy impact fracture surfaces of different aluminium alloy plates.

The residual velocity has been plotted against the tensile strength of the aluminium alloy target plates, (Fig. 7.5a). It can be seen that the residual velocity decreases with increase in tensile strength of the target plates. The kinetic energy absorbed by the different aluminium alloy target plates during ballistic testing is calculated as per Equation 2.1 and is shown in Fig 7.5 (b).The highest energy absorption is observed in case of AA 7017 target plates. At the same time, the lowest energy absorption is observed in AA 6061 plates among the studied aluminium alloys. The impact craters are sectioned in to half after ballistic testing

and are shown in Fig. 7.6. There are no cracks observed visually in the crater region of any of the aluminium alloy plates.

7.2.5. Post ballistic microstructural characterisation

The impact craters of all the aluminium alloy plates are investigated in detail after ballistic testing to observe the changes in microstructure. The post ballistic microstructures of the aluminium alloy plates are illustrated in Fig.7.7-7.9. In all the aluminium alloy plates material flow lines bent in the opposite direction of projectile motion along with large material deformation is observed. Small cracks are detected in the crater of AA 2519 target plates. ASBs are seen in the crater region of all the aluminium alloy target plates. However, lesser ASBs are noticed in the crater of AA 6061 target plates.

7.2.6. Post ballistic micro-hardness measurements

Micro-hardness measurements are taken at a load of 100 gm starting from close to the crater wall and gradually moving away. The variation in micro-hardness values in all the studied aluminium alloy target plates are shown in Fig. 7.10. In all the aluminium target plates, there is an initial rise in the hardness value and then it decreases with distance from crater wall.

7.3. Discussion

The alloys AA 2024, AA 2519, AA 6061 and AA 7017 belong to the series of heat treatable aluminium alloys. In contrast, AA 5059 and AA 5083 belong to the series of work hardenable aluminium alloys. As has been described in Chapters 5 the heat treatable aluminium alloys obtain their optimum properties through aging process where the formation of coherent precipitates enhances the strength and hardness of the material. The AA 5059 and AA 5083 alloys achieve their properties through alloying elements and the application of strain-hardening by heavy rolling operation (Crouch, 2016). The amount of alloying additions and morphology of precipitates play an important role in the strength and hardness of the aluminium alloys. From Table 2.1 it can be noticed that the AA 7017 alloy has the

(a)

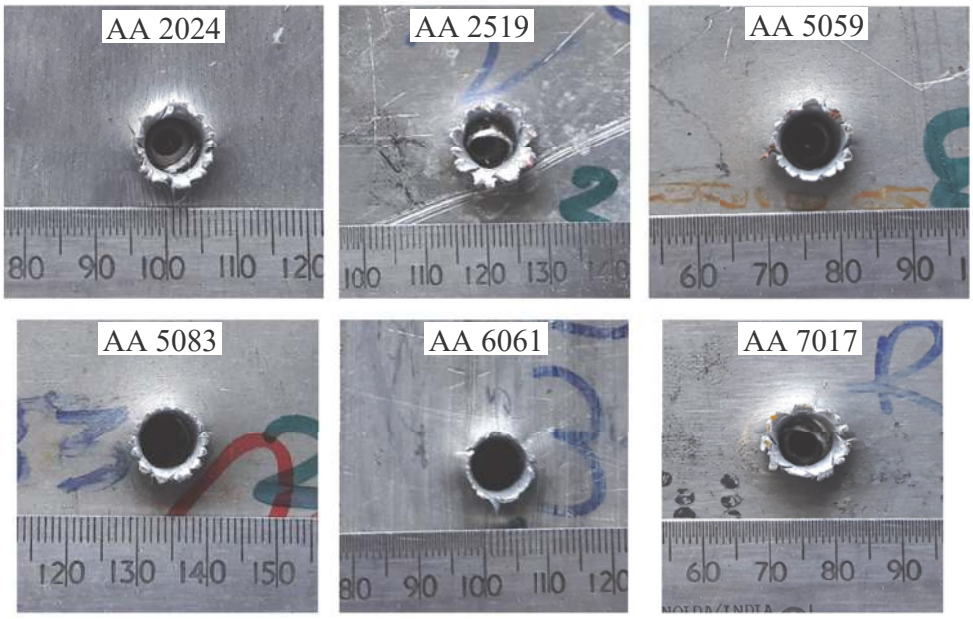

(b)

Fig. 7.4: (a) Front face of the aluminium alloy plates after ballistic impact, (b) Close up view of the damage patterns.

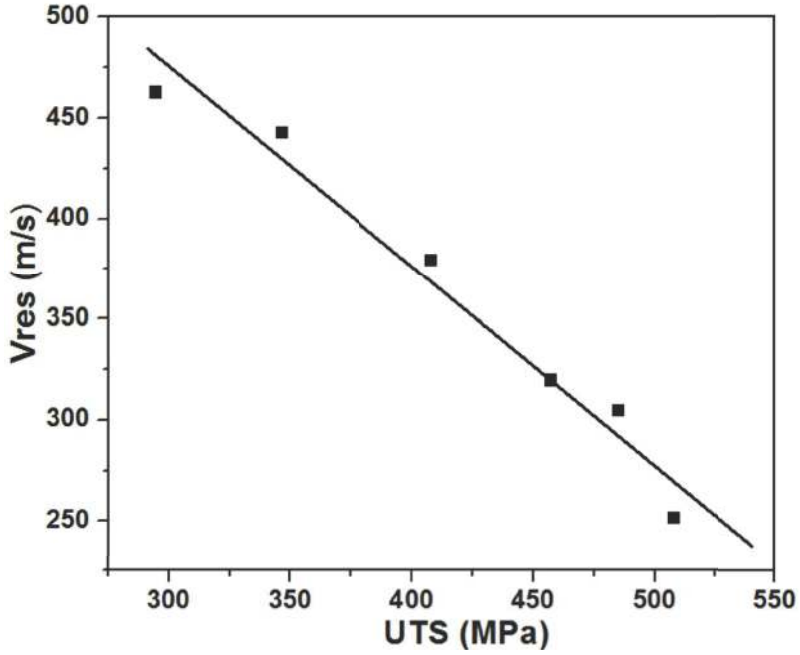

(a)

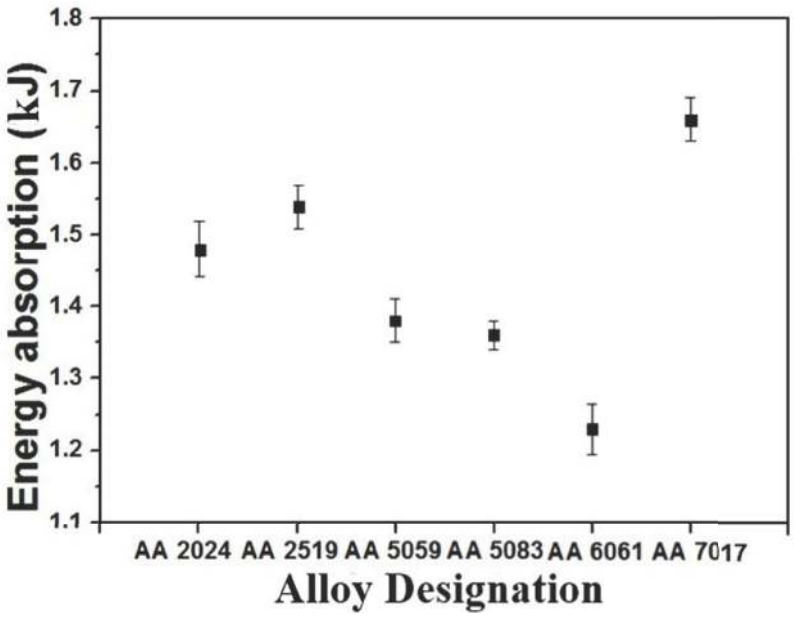

(b)

Fig. 7.5: (a) Residual velocity (Vres) with UTS of the target plates, (b) Kinetic energy absorption by different aluminium target plates.

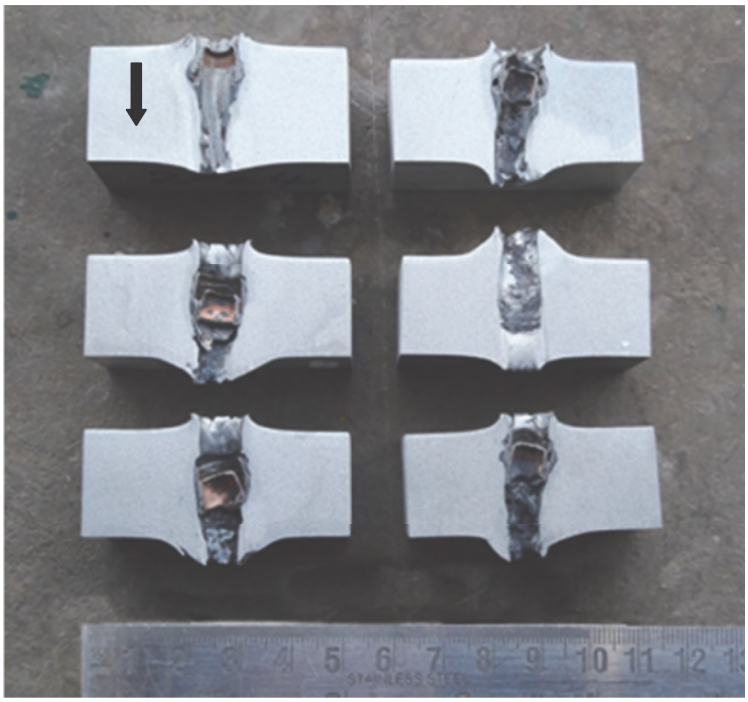

Fig. 7.6: Half section views of the impacted craters after ballistic testing. Arrow mark indicates the projectile penetration direction.

maximum amount of alloying elements in its composition. This explains the observation of highest strength and hardness in case of AA 7017 alloy. The AA 6061 has the lowest amountof alloying elements in its composition and hence, displays the lowest strength and hardness values. There is a limit up to which the strength and hardness can be increased by strain hardening process. Hence, AA 5059 and AA 5083 alloys exhibit lower strength and hardness in comparison to AA 2024, AA 2519 and AA 7017 aluminium alloys. It has been reported that heat treatable aluminium alloys demonstrate higher strength and hardness than those of work hardening aluminium alloys (Crouch, 2016).

Charpy impact energy values give a good indication of the resistance to failure of a material to a sudden applied force and are generally correlated with the ballistic behaviour of materials. This dimple like morphology clearly indicates a ductile failure mode. Ductile modeof failure implies extensive plastic deformation and energy absorption before fracture

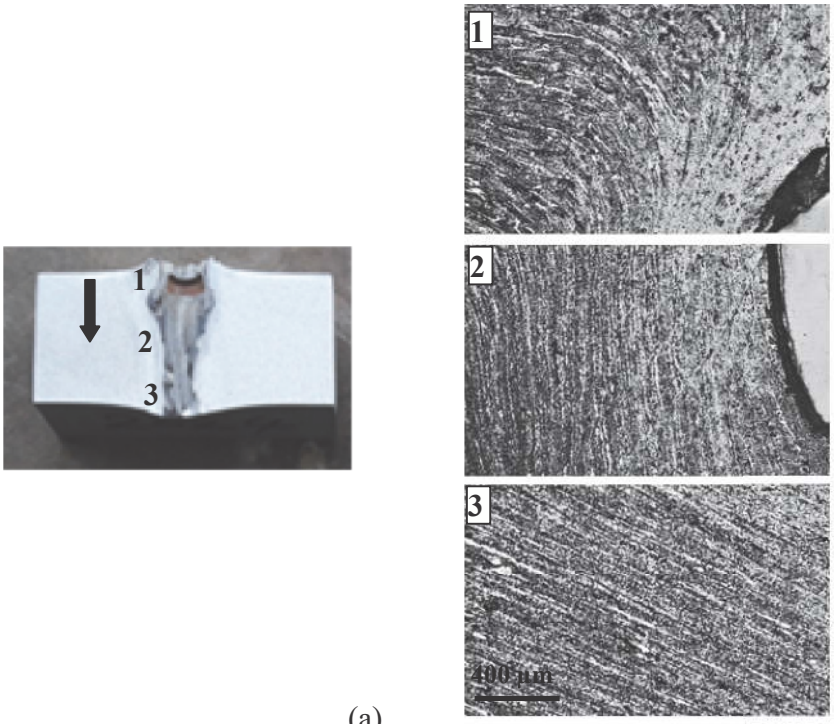

(a)

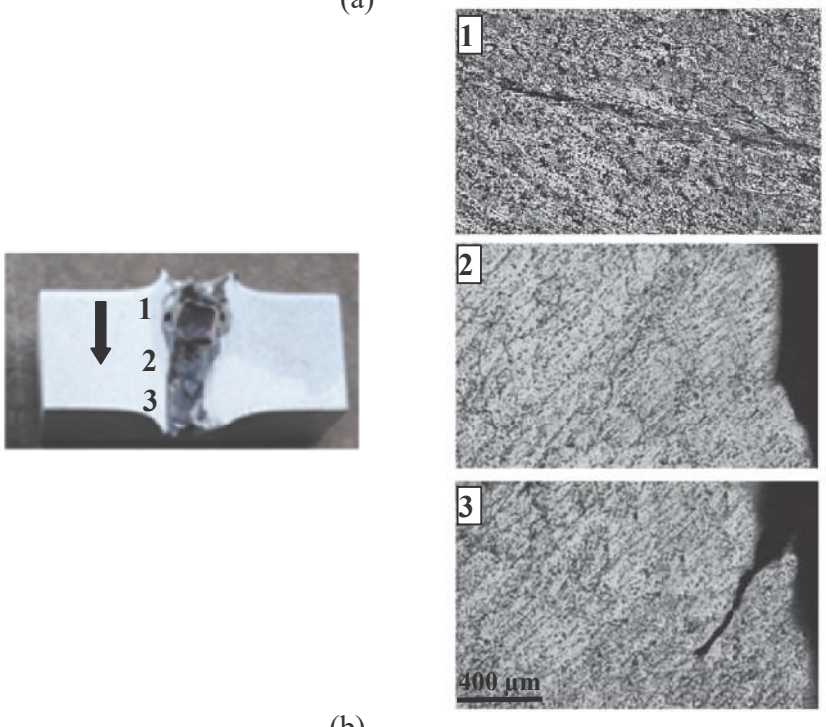

(b)

Fig. 7.7: Post ballistic microstructure adjacent to the crater wall of (a) AA 2024 (b) AA 2519 target plates. Arrow mark indicates the projectile penetration direction. The numbers in the microstructure indicate the corresponding region in the crater wall.

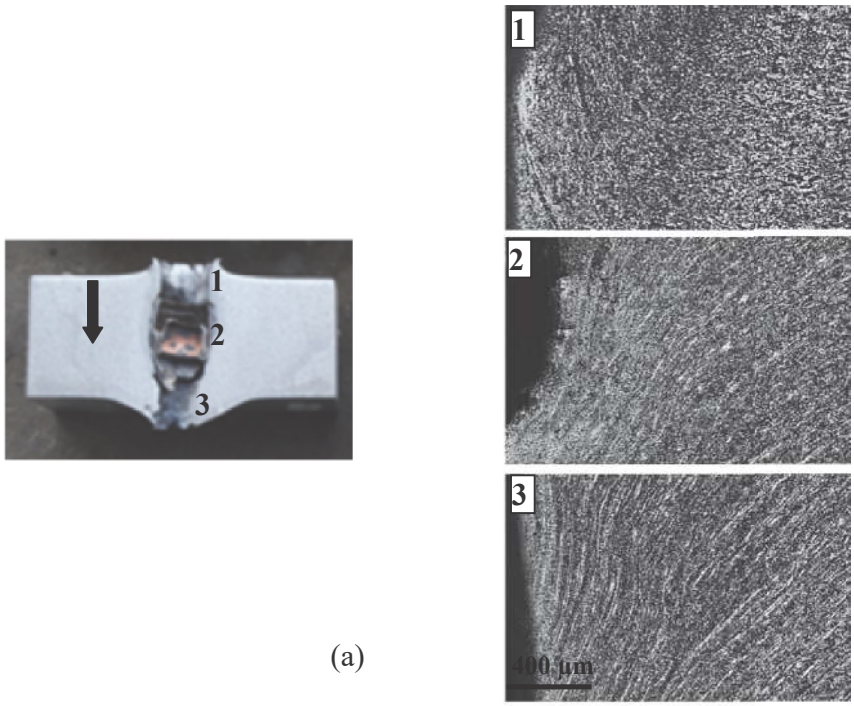

(a)

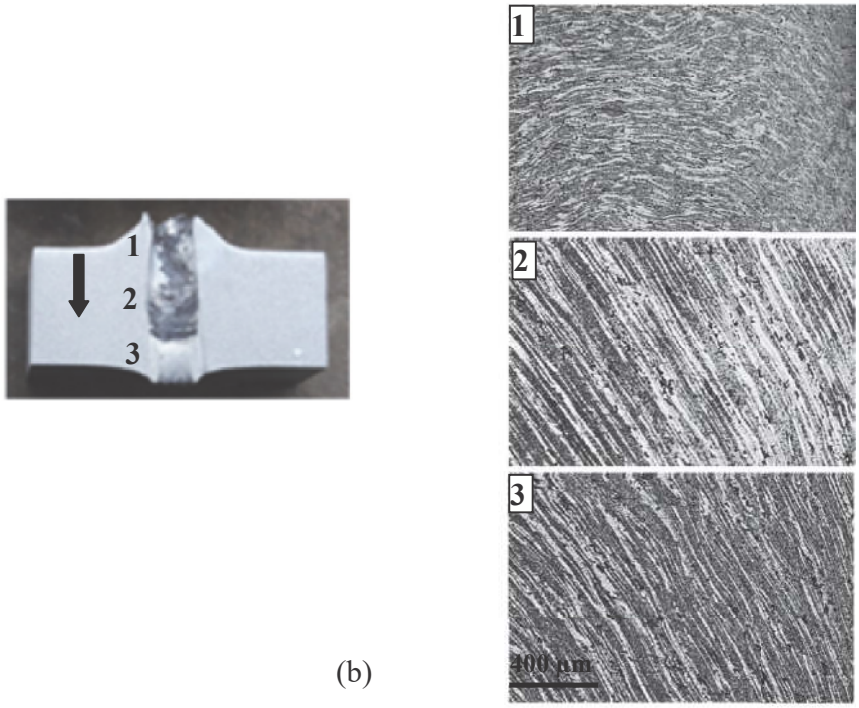

(b)

Fig. 7.8: Post ballistic microstructure adjacent to the crater wall of (a) AA 5059 (b) AA 5083 target plates. Arrow mark indicates the projectile penetration direction.The numbers in the microstructure indicate the corresponding region in the crater wall.

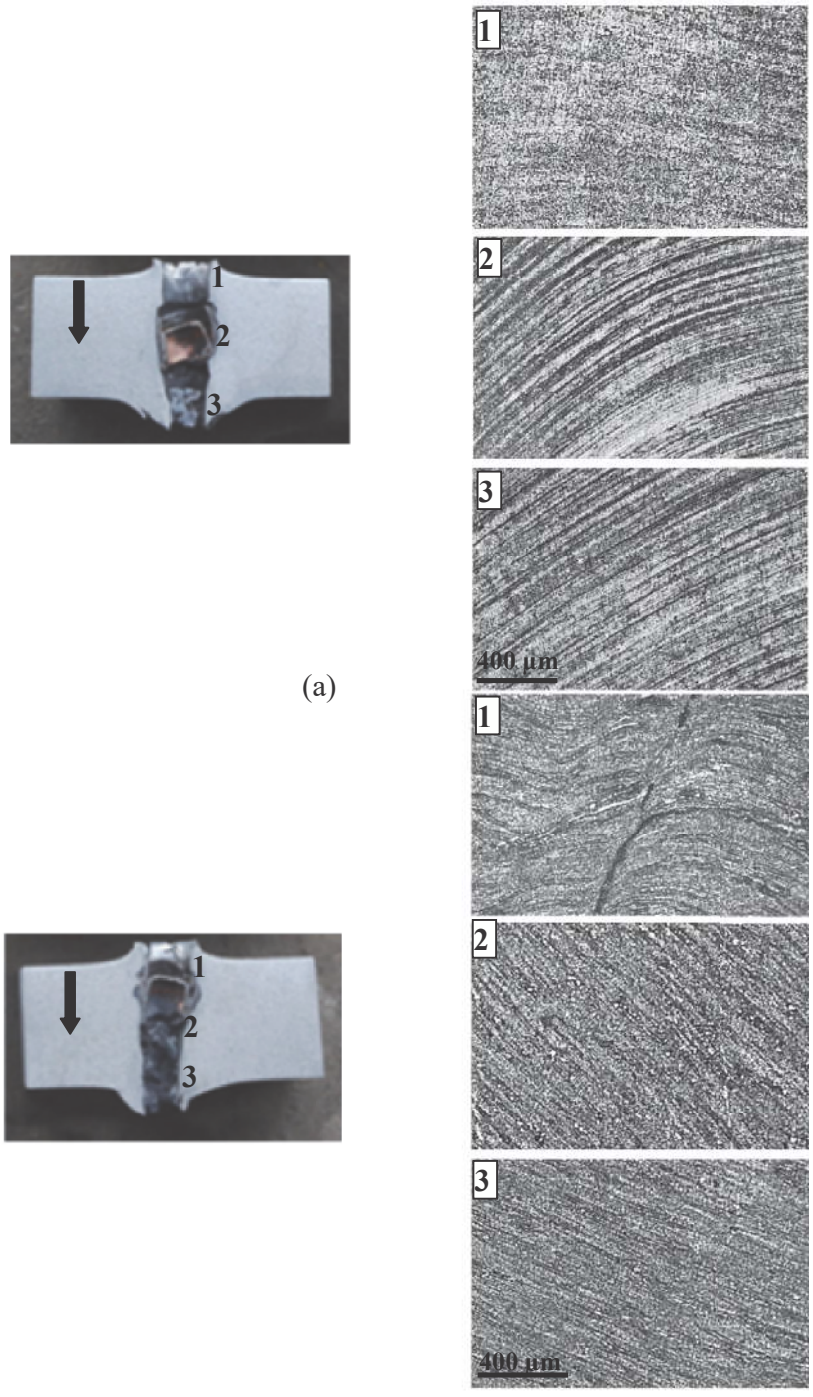

Fig. 7.9: Post ballistic microstructure adjacent to the crater wall of (a) AA 6061 (b) AA 7017 target plates. Arrow mark indicates the projectile penetration direction. The numbers in the microstructure indicate the corresponding region in the crater wall.

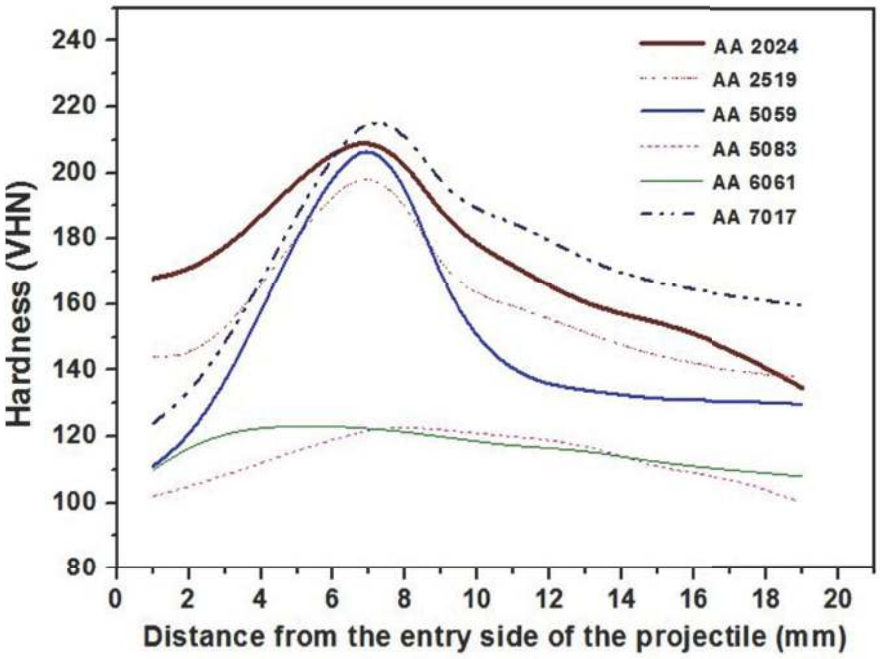

Fig. 7.10: Post ballistic micro-hardness measurements adjacent to the crater wall of different aluminium alloy plates.

and is a desirable criterion for armour materials.The difference in impact energy of the different aluminium alloys can be explained from their respective fracture surfaces (Figs. 7.3). As mentioned above, fine and shallow dimples in AA 6061 plates facilitate in absorbing the kinetic energy in an efficient manner. Hence, AA 6061 plates exhibit the highest Charpy impact values among the studied aluminium alloys. The coarse dimples seen in the fracture surface of AA 2519 plates decreases the energy absorption and hence a reduction in the Charpy impact values.

The energy absorption by different aluminium alloy plates during ballistic impact can be depicted from the post ballistic microstructural observations. The target material tries to absorb the kinetic energy from the projectile during ballistic impact. This results in the observation of deformed material and distorted material flow lines adjacent to the crater region. High Charpy impact energy assists in dissipation of the impact energy over a larger volume of the material and hence a homogeneous deformation is observed. However, at low

Charpy impact energy value, an inhomogeneity in deformation is observed. This causes the formation of ASBs. Formation of ASBs has already been described in previous Chapters (Chapter 3 and 4). The cracks observed in the post ballistic microstructure of AA 2519 craters can be correlated to its lowest Charpy impact values. The hardness values adjacent to the crater wall indicate the extent of deformation during ballistic impact. As has been stated previously the variation in hardness adjacent to the crater region is a result of annealing and strain hardening caused by projectile impact.

It has been pointed outpreviously that ballistic resistance increases with increase in material properties like strength and hardness. Consequently, the AA 7017 target plates display the best ballistic performance owing to its highest strength and hardness values among the studied aluminium alloys. The results are in line with the previous studies (Borvik et al.,2009).

7.4. Conclusions

The AA 7017 alloy exhibits the best ballistic performance among the studied materials. Ballistic penetration resistance of the present alloys is in accordance with their strength and hardness values. It appears that the strength and hardness values are more dominant parameters against small calibre ammunitions.